A multi-objective energy management optimization for a hybrid electric bus covering an urban route

Bernardo Tormos, Benjamín Pla, Pau Bares and Douglas Pinto

Abstract

The development of electrified vehicles is a promising step toward energy savings, emissions reduction, environmental protection, and more sustainable economic growth. In the case of hybrid electric vehicles (HEVs), the energy management strategy (EMS) is essential for their efficiency and energy consumption. Typically, EMS employs rule-based strategies calibrated to general driving conditions. So, this paper proposes to calibrate the EMS of an urban hybrid electric bus that covers a particular route by taking advantage of past driving information. The EMS computes the percentage of the vehicle power demand that must be supplied by each of the sources (fuel and battery) and also controls the heating, ventilating and air conditioning (HVAC) system to achieve cabin thermal comfort. The proposed approach is based on employing an optimal solution by dynamic programming in a previous loop covered by the bus in the considered route. Then, the cost-to-go matrix is stored and used in the following trips by applying the one-step look-ahead rollout, taking profit from the similarities of the loops in the route. To compare and evaluate the performance of the proposed algorithm, a benchmark was carried out by employing the widespread equivalent consumption minimization strategy (ECMS) approach, combined with rule-based strategies in the HVAC control system. Finally, the pareto front presents the trade-off between cabin temperature control performance and total fuel consumption, allowing to compare and evaluate the different EMS calibrations.

Keywords

HVAC, EMS optimization, HEV control

1 Introduction

Despite policy efforts to encourage the development of more efficient technologies in the transport sector and renewable energies, this sector has the most significant dependence on fossil fuels and was responsible for 37% of CO2 emissions from end-use sectors in 2021[1]. To overcome these issues, the employment of electrified powertrains, such as battery electric vehicles (BEV), hybrid electric vehicles (HEV), has shown to be an essential step to reduce energy consumption and emissions[2]. HEV increases the possibility of reducing fuel consumption and emissions compared to traditional ICE-based vehicles due to the combined use of two energy sources, internal combustion engine (ICE) and battery[3]. So, this integration of multiple power sources requires an efficient energy management strategy to match the efficient operation of the system.

The improvements of HEV can be explored by modeling a powertrain topology that best fits the vehicle application or sizing the components[4,5]. However, choosing an appropriate control strategy for HEV applications also plays a key role in the optimal and efficient operation of these multiple energy sources[6]. Furthermore, when assessing factors that affects the overall energy consumption of a vehicle, it is essential to consider not only the energy required for propulsion but also the auxiliary loads. Among these loads, the Heating, Ventilation, and Air Conditioning HVAC system emerges as one of the most significant contributors to battery usage in electrified vehicles, accounting for up to 30% of the total energy consumption under specific conditions[7]. So it is essential to consider the HVAC power consumption related to the cabin temperature control to guarantee the passengers comfort and energy efficiency.

To fully explore the potential of an HEV, the EMS is essential to control the energy flow within the vehicle. It aims to minimize fuel consumption while fulfilling the driving power demands and constraints, such as the maximum power limitations and battery state of charge that should be maintained in a certain range[3]. This topic has been extensively discussed in the literature, and a comprehensive review can be found in[8]. Moreover, it should be noted that the performance and optimal energy management strategy (EMS) are influenced by various factors, including driver behavior, road slope, and traffic conditions[9].

Authors usually categorize the EMS in different arrangements, but two of them can be highlighted: ruled-based and optimization-based.[10]. First, ruled-based strategies are usually based on heuristic approaches, employing high calibration efforts to consider the different set of operating conditions that the vehicle can face[11].

CMT – Motores Térmicos, Universitat Politécnica de Valéncia, Valencia, Spain

Corresponding author:
Douglas Pinto
Email: dpdouube@upv.edu.es

The optimization-based methods can be applied to offline approaches, e.g., design or benchmarking with developed strategies, and also for online control purposes, depending on the information available [10].

Regarding optimization-based methods, optimal control can be applied to the energy management problem of an HEV, where a model is employed to evaluate a predefined cost function that can estimate the impact of the control decisions [8]. The offline optimization often requires that the driving cycle and disturbances related to the problem are well known in advance, which just happens in homologation cycles or specific applications. The most spread techniques employed in these optimization problems are Dynamic Programing (DP) [12] and Pontryagin's Minimum Principle [13]. DP is a powerful optimization technique widely applied to HEV energy management. It is used for offline optimization, where the solution is usually used as a benchmark with other approaches, or for developing EMS or advanced HEV control strategies [10]. First, the state and control variables grid is constructed based on the system input parameters. Subsequently, the DP algorithm assesses the cost and state transitions associated with each control policy, considering all states in a backward over time. As a result, the optimal cost-to-go function is stored depending on states and control actions, allowing for a comprehensive evaluation of the entire problem. The optimal solution is then determined by selecting the path with the lowest cost-to-go [14].

In order to overcome the driving cycle dependence of these optimal control tools, several researchers have been developing online optimization-based methods. Some of them are based on the Equivalent consumption minimization strategy (ECMS) [15], where the selected control action is the one that minimizes a cost function related to the energy consumption of the fuel tank and the batteries. Moreover, there are several adaptations of this method in the literature, called adaptive ECMS [16,17]. These methods rely on using various information sources to dynamically adapt the equivalent factor in response to driving conditions. A further approach for addressing the driving cycle dependency is model predictive control (MPC) [18]. This method can estimate future driving conditions based on some information available (e.g., traffic lights, preceding vehicles, and road slope) while fulfilling the system constraints.

However, implementing MPC in real-time applications for HEVs poses several challenges, including hardware limitations, constrained processing power, and communication delays. The increased computational costs of such approaches stem from solving optimization problems repeatedly over a finite prediction horizon [19]. The selection of this horizon is critical, as a longer prediction horizon improves performance by considering future states and constraints that affect control performance and computational complexity. Additionally, control-based approaches like MPC and ECMS require some form of prediction of future conditions. For instance, MPC requires future predictions to provide the optimal control policy directly. At the same time, ECMS relies on predicting future conditions to calibrate the weighting parameter between the battery and Internal ICE costs, respectively.

The optimization of energy management strategies in HEV can be extended to incorporate the energy consumption of HVAC system, which can account for more than 30% of the maximum battery power [20]. Additionally, the HVAC control optimization can reduce the total energy consumption of electrified vehicles by approximately 14%, as observed under simulation conditions by [21]. For instance, [22] presented a sequential optimization for eco-driving speed trajectory planning, air conditioning thermal load planning, and powertrain control in a hybrid electric vehicle in a connected and automated vehicle environment. Results show that the complete optimization strategy could improve energy consumption by up to 18.8%.

Authors in [23] developed a two-layer MPC that employs the vehicle speed and traffic predictions to compute the optimal trajectories for the cabin and battery cooling in HEV. Later, using these trajectories in the energy management controller to compute the proper power split. A neural network model predictive control is proposed by [24] to control the HVAC system of a battery electric bus. The results show that the proposed method could reduce close to 2.8% in total energy consumption compared with standard strategies compound by PID controllers. Furthermore, the characteristics of the predicted horizon in HEV integrated power and thermal management approaches were investigated in [25]. The authors discuss the computational burden, accuracy, and resolution of look-ahead information employed in a multi-horizon MPC-based strategy.

As observed in the literature, the problem of integrated energy management strategies in electrified vehicles usually relies on estimating future driving conditions, thermal loads on batteries and cabins, or information available from connected and automated vehicle environments. This paper proposes an online applicable strategy for controlling the air conditioning system and power split of a hybrid electric urban bus. The EMS takes advantage of the particular application, i.e., an urban bus, where the route is repeated so the future driving conditions can be reasonably well predicted with past driving cycles. So, the cost-to-go matrix obtained by offline DP optimization is generated by evaluating a simplified bus model and overcoming increased computational efforts related to predictive approaches widely applied to online control purposes. Later, this matrix is employed in the EMS of the bus on the consecutive loops to be covered. The goal is to reduce the total energy consumption of the integrated HVAC system while keeping the vehicle operating in charge-sustaining mode. However, the proposed strategy is not limited to the optimization of HEV, it also can be extended to other applications that exploits daily commute trips or similar driving conditions.

2 Case Study

This case study considered a hybrid electric urban bus that covers the same route daily. The driving cycle information was acquired from the Valencia public transport service (EMT-Valencia). The evaluated data contains information of two consecutive working days of the route (“Universitats-Hosp.Dr.Peset”), containing a total of 287 km covered. Each vehicle journey is approximately 15.1 km long and is completed 9 and 10 times in the two days analyzed, accounting for 284 km traveled. The average journey time is 5100 seconds with a standard deviation of 320 seconds. The vehicle position was provided by the GPS, while the vehicle speed profile by the bus OBD port. The GPS signal determines the ending point and the starting point of next loop, then, once the bus reach the ending point, the vehicle speed is integrated providing the distance covered in the loop.

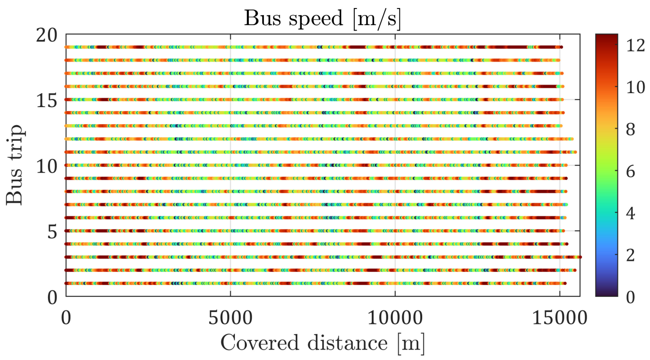

Figure 1. Measured vehicle speed of the bus on the specific route, representing the 19 loops covered in two consecutive days.

Fig. 1 shows the vehicle speeds as a function of the vehicle position along the route for the 19 loops. In a previous work, a discussion about the bus driving cycles of the selected route was carried out[26]. The study concluded that the bus speed traces exhibit similar patterns across different positions along the route. Notably, it can be inferred that the disturbances experienced in each loop are similar, given that the routes encounter the same traffic lights, stops for embarking and disembarking passengers, and speed limits. However, some variations in the total distance covered by the bus in the loops can be observed. These discrepancies may arise from differences in driving trajectories and maneuvers to avoid obstacles or measurement uncertainties.

The total passenger number can affect the cabin temperature, significantly impacting the total heat load[20]. The bus line covers a route that connects a university situated at one end of the city to another end, passing through the central region and including 36 bus stops. The estimated distribution in the number of passengers is shown in Fig. 2.

3 Plant description

To evaluate the control strategies, a complete vehicle model plant was built in GT-Power. This system contains the complete vehicle dynamics, air conditioning system and cabin model. The selected architecture of the HEV bus follows the P2 construction shown in Fig. 3. The main HEV bus model characteristics are outlined in Table 1. In the considered hybrid configuration, the electric motor and the internal combustion engine are connected through an axle, which is directly connected to the transmission, then connects through a differential to the vehicle wheels.

Note that the complete HVAC model is connected to the high-voltage battery of the hybrid powertrain, so the

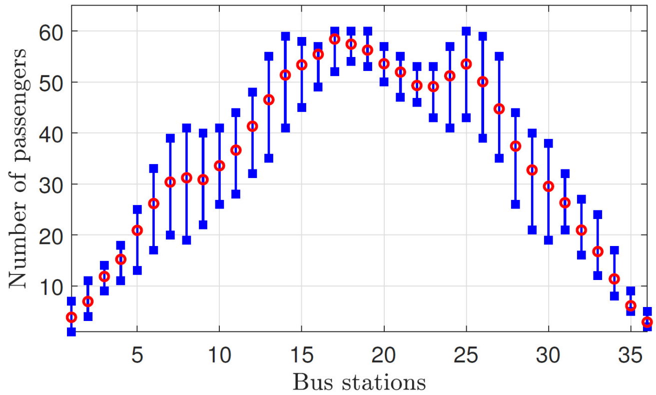

Figure 2. Average, maximum, and minimum estimated number of passengers in the bus for the 19 analyzed cycles, distributed in 36 bus stops.

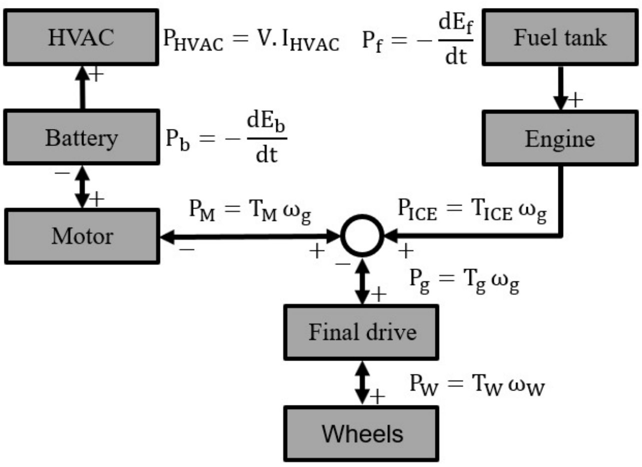

Figure 3. Parallel HEV architecture employed on the problem and power sign criteria through the system components

energy consumed in the HVAC system is provided by the high-voltage battery. The battery can recover energy through regenerative braking or from the combustion engine operating in hybrid mode. On the other hand, energy is consumed when the electric motor assists the combustion engine in propelling the vehicle and providing the power for the HVAC system.

Table 1. Description of the HEV bus model main characteristics.

Parameter	Value
`Weight`	15000 kg
`Frontal area`	7.24 m^2
`Drag coefficient`	0.78
`Motor rated power`	150 kW
`Engine rated power`	200 kW
`Battery capacity`	11.8 kWh

The HEV bus considered in this case study is exposed to summer conditions due to the critical working conditions in the region, which means that the HVAC system operates in cooling mode, then rejects heat from the cabin to the ambient. The model used to represent the thermal balance, and the cabin temperature was the lumped cabin model (0D). However, a 1D model was employed to model the air conditioner coolant circuit. Fig. 4 shows the parameters and

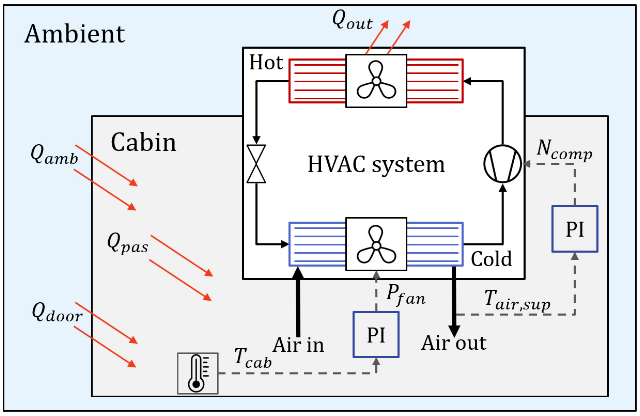

Figure 4. Simplified representation of the cabin plant model and the standard control of the HVAC system.

surrounding conditions that affect the cabin temperature. The air entering the cabin exchanges heat with internal components and is then recirculated through the cold side of the AC system. All features, such as windows, seats, and surface materials, are related through heat exchange properties and affect the cabin temperature. As well as the heat generated by the number of passengers Q_{pas} and the heat added by the doors opening at the bus stations Q_{door} represent most of the heat added to the cabin. The general passenger heat load is estimated as[27] and is characterized by Eq. (1).

$$Q_{pas} = N_{pas} h_{pas} \tag{1}$$

Where N_{pas} represents the number of passengers inside the bus, and the h_{pas} (W) is the heat generation per passenger, this value is related to the human body metabolic rate and the average skin area, but in this work, this value was considered constant for all passengers and equal to 170 W[28]. Also, Eq. (2) estimates the impact of the door opening at bus stops and is modeled according to[29]. This additional heat added to the system is applied for 30 s, time considered necessary each time the bus changes the number of passengers at a bus stop.

$$Q_{door} = \rho_{air} C_p (T_{amb} - T_{cab}) V_{inf} \tag{2}$$

where ρ_{air} (kg/m^3) and C_p (kJ/kg K) are the air density and specific heat, T_{amb} (ºC) and T_{cab} (ºC) the air ambient and cabin temperature and V_{inf} (m^3/s) is the air infiltration flow rate:

$$V_{inf} = C_A A_{door} \sqrt{R_p} \tag{3}$$

being C_A air flow coefficient (m^3/s)/(m^{2}Pa$^{0.5}$), A_{door} the total area of the door when opened (m^2) and R_p the pressure factor (Pa).

The original system comprises rule-based control strategies and PIs to control the HVAC system aiming to maintain the cabin temperature at the desired setpoint. These control actions were applied in the standard method. As shown in Fig. 4, the PI of the AC compressor controls the compressor speed N_{comp} to keep the air temperature of the supplied air at 5 ºC. Also, a PI controller is employed to control the air flow rate of the cold side of the system to maintain the cabin temperature close to the setpoint. On the other hand, the standard PI that controls the compressor speed was replaced by the direct input computed by the proposed strategy, and this method will be explained in previous section. In addition, other components and parameters relevant to the air conditioning system circuit were unchanged for both approaches.

4 Control-oriented model

The model used to represent the vehicle powertrain is based on longitudinal vehicle dynamics. So, according to the hybrid architecture in Fig. 3, the power demand to move the vehicle in the driving cycle is equal to the power provided by the power split. So as the motor and the ICE are connected in the same shaft, they share the same speed, thus, the relation between the torque provided by the motor T_m and the ICE T_{ICE} must be equal to the torque in the powertrain transmission T_g:

$$T_g = T_m + T_{ICE} \tag{4}$$

For each time step, the torque demand to drive the vehicle is computed by:

$$T_w = (m\dot{v} - mg\mu cos\theta - mgsin\theta - \frac{1}{2}\rho A c_d v^2) R_w \tag{5}$$

where m is the equivalent vehicle mass, v, $\dot{v}$, g is the vehicle speed, acceleration and acceleration of gravity, respectively. Also, ρ is the air density, Ac_d the product of the bus frontal area and aerodynamic coefficient and R_w the wheel radius. Finally, the μ is the rolling coefficient, θ is the angle due to the road slope, which is neglected in the considered problem. While the motor and ICE speeds are proportional to the wheel speed via the specified gear ratio, their joint torque T_g in Eq. (4) is proportional to the wheel torque via the inverse of the gear ratio. So, if the demanded vehicle speed is known, the vehicle acceleration and T_g may be determined using Eq. (5) and the gear ratio. Consequently, Eq. (4) may be rewritten by specifying the control action as $u = T_m$:

$$T_{ICE} = T_g - T_m \tag{6}$$

then, the ICE torque is computed given the vehicle-speed demand and decision u known. With respect to the ICE model, it is based on the quasi-static technique developed in[30], which employs experimental data to map the fuel consumption m_f as a function of engine speed ω_g and torque T_{ICE}:

$$m_f = g(\omega_g, T_{ICE}) \tag{7}$$

The dynamic equation that governs the energy stored in the battery (E_b) is given by:

$$\dot{E}_b = -P_b \tag{8}$$

where P_b is the battery power, positive when the battery is drained, and negative when being charged as represented by the signs in Fig. 3. Note that P_b depends on the HVAC power consumption P_{HVAC} and the motor power P_m according to the following equation:

$$P_b = P_{HVAC} + P_m \tag{9}$$

The P_m uses a quasi-static map to obtain the efficiency depending on the ω_g and T_m. Equally, a simple map based on the compressor speed is employed to estimate the P_{HVAC}. Finally, the battery is modelled with an electrically equivalent circuit based on resistance in series with a voltage source:

$$V = V_{oc} - I_b R_b \tag{10}$$

where I_b is the battery current, and R represents its internal resistance that depends on the battery state of energy SoE, i.e., a measure of the battery energy level concerning the total energy content of the fully charged battery $E_{b,0}$:

$$E_{b,0} = V_{oc,0} Q_{b,0} \tag{11}$$

with $V_{oc,0}$ and $Q_{b,0}$ being the open circuit voltage and charge of the fully charged battery. The actual energy stored in the battery is represented by:

$$E_b = V_{oc} Q_b \tag{12}$$

So, normalizing the battery energy, the state of energy of the battery can be defined as:

$$SoE = \frac{E_b}{E_{b,0}} = \frac{V_{oc} Q_b}{V_{oc,0} Q_{b,0}} = SoC \frac{V_{oc}}{V_{oc,0}} \tag{13}$$

where SoC is the battery state of charge, used in many works instead of the SoE.

A simplified model of the HVAC system implemented in the GT-Power bus plant comprising the lumped cabin model (0D) and the coolant circuit (1D) is necessary for two reasons. First, the complexity of the resulting system modelled increases the computational effort to evaluate the different control actions in the control-oriented model used in real-time optimization. Second, as the proposed strategy employs a DP approach, increasing the states of the optimal control problem increases the system complexity, requiring high computational demands. So, to obtain a simple model of this complex system, a linear model was developed by investigating a set of variables and parameters that exhibit correlations with the original system.

The Eq. (14) represents the simplified discrete time model of the cabin temperature. For a given time step, the estimated T_{cab} is affected by the disturbances; Q_{pas}, Q_{door},T_{amb}, the state T_{cab} and the control action N_{comp}. The sub-index k expresses the current time-step and α_n the model parameters to be calibrated with the responses from the plant. The data evaluated to calibrate the α_n parameters were two consecutive loops, where the control strategy employed in the HVAC system was based on PIs controllers.

$$\begin{aligned} T_{cab_{k+1}} = \alpha_1 T_{cab_k} - \alpha_2 N_{comp_k} + \alpha_3 (N_{comp_k})^2 + \\ \alpha_4 (Q_{pas_k} + Q_{door_k}) + \alpha_5 (T_{amb_k} - T_{cab_k}) \end{aligned} \tag{14}$$

The positive signals attributed to the terms in Eq. (14) represent the parameters that contribute to the heat load on the cabin. In contrast, the negative terms can reject heat from the cabin to the ambient,i.e., the compressor speed only. Note that the term representing the temperature difference between the environment and the cabin, to some extent, compasses the heat exchanges between the walls, floor, windows, and other bus components. It was also observed that in conditions with a high number of passengers on the bus, the model responds differently because the principal source of heat added to the cabin is provided by the passengers. So, to overcome this issue, a threshold was defined, and the parameters were adjusted in a dual-zone model. Similarly, a model to represent the HVAC power consumption was developed. The model is necessary to estimate P_b, which depends on the P_{HVAC}:

$$P_{HVAC_{k+1}} = \gamma_1 N_{comp_k} - \gamma_2 (N_{comp_k})^2 + \gamma_3 \tag{15}$$

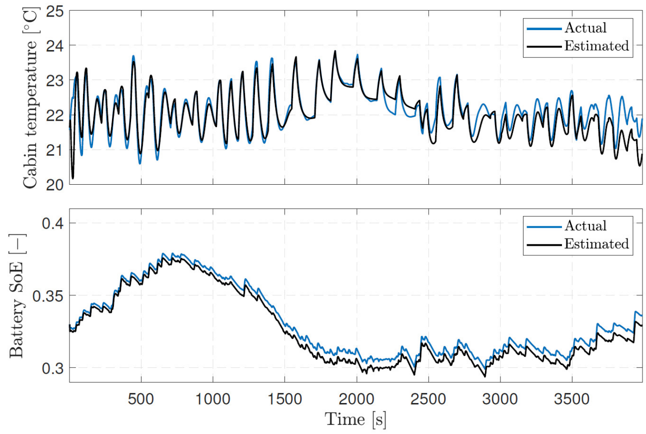

Figure 5. Model validation: Comparison between actual cabin temperature and battery SoE of the plant model and the estimated with the simplified model for one bus trip.

Fig. 5 shows the validation of the control-oriented model, where a comparison is presented between the estimated problem states (SoE and T_{cab}) and the actual provided by the HEV plant under the influence of identical inputs (P_{HVAC} and P_m) in one bus trip. It can be observed that the SoE and T_{cab} estimations accurately reproduce the results with minimal deviation from the actual state. Note that the estimated results are obtained without feedback on the actual system condition. However, in the proposed control strategy, there will be feedback on the SoE and T_{cab}, and then these small discrepancies will be even reduced once the error is not integrated over time. This way, the parameters of the linearized model are presented in Table 2. After evaluating multiple models of varying orders, the selected model provided a good compromise between accuracy and complexity.

Note that the present work does not consider any couple between the HVAC system to the battery thermal behaviour, their cooling systems are modelled separately. Given the significance of summer conditions in Valencia, the study focuses on the HVAC operating in cooling mode. Consequently, battery temperature is not critical in this case and was not considered in the EMS optimization. Future work will consider a more complex control-oriented model that considers the thermal management of the connection between the battery pack, ICE, and HVAC system, probably with a more significant number of states.

5 Optimization problem

The primary objective of EMS optimization is to minimize energy consumption while satisfying the driver power

Table 2. Simplified cabin model coefficients

Coefficients Value	[Npas≤50]	[Npas>50]
α_1	0.9722	0.9773
α_2	0.000342	0.000201
α_3	5.308e-08	2.723e-08
α_4	0.000306	0.000263
α_5	0.0368	0.0239
γ_1	3.0013	3.0013
γ_2	2.552e-04	2.552e-04
γ_3	1.329e+03	1.329e+03

request and maintaining cabin thermal comfort. To achieve this goal, the following cost function is introduced:

$$J = \Phi(x(t_f)) + \int_{t_0}^{t_f} L(x(t), u(t), w(t))dt \tag{16}$$

where t_0 and t_f are the initial and final time of the cycle, x is a vector containing the system states, u represents the control actions, and w represents disturbances that impact the system evolution, such as ambient temperature T_{amb}, Q_{pas}, Q_{door}, and v. This equation includes a terminal cost Φ related to t_f, penalizing deviations from the desired final state, in this case, the energy stored in the battery. Additionally, the term L represents the instantaneous cost function, relating fuel consumption P_f and the squared deviation of cabin temperature T_{cab} from the setpoint T_{set} over the covered loop, as expressed by:

$$L = \beta P_f + (1 - \beta)(T_{cab} - T_{set})^2 \tag{17}$$

So the multi-objective optimization proposed by this paper is addressed by the term β, which assigns importance to each parameter in the optimization process. This parameter remains constant and is varied to study its impacts on cabin temperature control performance and total energy consumption, further discussed in the Results and discussion section. The corresponding optimal control problem is mathematically described by:

$$u^* = argmin_u \int_{t_0}^{t_f} J(\mathbf{x}, \mathbf{u})dt \tag{18a}$$

subject to:

$$\dot{x} = f(\mathbf{x}, \mathbf{u}) \tag{18b}$$

$$E_{b,0} \cdot 0.3 < E_b < E_{b,0} \cdot 0.7 \tag{18c}$$

$$T_{cab,min} < T_{cab} < T_{cab,max} \tag{18d}$$

$$\Phi = \sigma_{cost}(SoE_{t_f} - SoE_{t_0})^2 \tag{18e}$$

The system dynamics (18b) corresponds to the battery and cabin temperature dynamics with state vector:

$$\mathbf{x} = [SoE \; T_{cab}]^T \tag{19}$$

To achieve energy consumption minimization, the EMS must compute the optimal settings for the decision variables:

$$\mathbf{u} = [T_m \; N_{comp}]^T \tag{20}$$

Three constraints were incorporated to address the problem discussed in this paper. Eq. (18c) sets the maximum and minimum range limits for the SoE, ensuring it remains within the bounds defined in Eq. (13). Specifically, the battery state of charge cannot fall below 0.3 or exceed 0.7 to prevent battery damage and overcharge. Equation 18d establishes limits for the cabin temperature throughout the cycle, ensuring it remains between 19 and 26 °C to maintain passenger comfort. Eq. (18e) introduces a terminal cost reflecting the difference between the initial and final conditions of the battery state of charge SoE_{t_0} and SoE_{t_f}.

5.1 Standard solution

The standard solution employed to solve the optimization problem presented in Eq. (16) is the equivalent consumption minimization strategy (ECMS). This strategy is based on setting a cost to the electrical energy stored in the battery by employing an equivalence factor λ in the battery power, so this energy is equivalent to using a certain quantity of fuel in the ICE. Therefore the integral problem can be replaced by the instantaneous minimization of the following expression:

$$C = P_f + \lambda P_b \tag{21}$$

the λ weights the cost of the two possible energy sources, one can note that high values assign a high cost to the battery usage, promoting the ICE usage and battery charging. On the other hand, low values impose a low penalty on battery usage, then providing fuel savings and depleting the battery energy. However, this method has a drawback, where for a given driving cycle, there is an optimal value of λ that minimizes fuel consumption and maintains the charge-sustaining operation, which need to be calibrated in conditions where the driving cycle is perfectly known in advance. So, to overcome this limitation, as the driving cycle is unknown, the λ can be calibrated in a reference cycle and then adapt the value depending on the operating conditions, as shown by[3,31]. In the present work, the λ is calibrated in a previous loop of the bus route and next applied in the following loops to be covered. Further, with feedback from the SoE, a correction is used when the SoE falls out of the desired range (0.3 and 0.7). Regarding the HVAC control, the original rule-based controller composed of the PIs was kept. Providing just the estimation of the P_{HVAC} to the ECMS controller to account for P_b.

5.2 Proposed solution

While perfect knowledge of the driving cycle is not available in real-time control applications, it has been observed that the various bus loops share similarities in the case at hand. Hence, the approach utilizes one of these loops to generate a DP optimization as an initial reference for energy management optimization. The rollout algorithm will be employed for this purpose[32].

According to Bellman's principle of optimality: "An optimal policy has the property that whatever the initial state and initial decisions are, the remaining decisions must constitute an optimal policy with regard to the state resulting from the first decisions"[33], from which it can be inferred that any partial path within the optimal one is also optimal between its initial and final states, then providing the Hamilton-Jacobi-Bellman (HJB) equation:

$$\mathcal{J}^*(x(t),t) = min_u \Bigg\{ \int_t^{t+\delta t} L(x(\tau),u(\tau),\tau) d\tau + \mathcal{J}^*(x(t+\delta t), t+\delta t) \Bigg\} \quad (22)$$

where the optimal cost-to-go $\mathcal{J}^*$ from any given state $x(t)$ at time t ($t_0 \leq t \leq t_f$) can be expressed as a sum of two intervals. The first one represents the cost of a differential problem with length δt and the second is the optimal cost-to-go from the resulting state at $t+\delta t$ to the end. The dynamic programming algorithm explores the Bellman principle of optimality and the HJB equation to numerically solve an optimal control problem. As this method is based on the discretization of the problem time in n time-steps, hence starting from any state value in a given time-step (k), Bellman's principle of optimality implies that:

$$\mathcal{J}^*(x,k) = min_u \{L(x,u) + \mathcal{J}^*(x,k+1)\} \quad (23)$$

To solve this problem, x and u spaces are discretized, then starting from the last time-step $k = n-1$ (so $\mathcal{J}^*(x,n) = \Phi(x(n))$) and proceeding backward accumulating the cost-to-go for the entire length of x and obtaining a resulted space of cost-to-go values for the optimal solution at the initial time-step as a function of the initial state $\mathcal{J}^*(x,1)$. So the potential of DP as a mathematical tool in the optimization of dynamic systems is that once the value of $\mathcal{J}^*(x,k)$ has been stored, it allows the evaluation of not only the optimal solution from the initial state but also from any particular point in (x,k) space. However, this potential suffers from the so-called curse of dimensionality. In the case of a high discretization applied to the states and actuators, it increases the number of combinations to evaluate during the problem solution. Consequently, generating high computational efforts to compute the problem solution.

To solve the optimization problem (Eq. 16), perfect knowledge of disturbances such as the bus speed profile, ambient temperature, and passenger information is necessary. However, since future driving conditions cannot be known beforehand, DP cannot be used for online control applications. In this context, one of the contributions of the paper is that instead of predicting the future driving cycle, past driving cycle information is used, exploring the benefits of repeated bus routes. This way, avoiding the online time-consuming optimization due to the long horizon of predictive approaches. So, this paper proposes pre-computing a DP solution offline for an arbitrary loop previously covered by the bus as a base policy for the EMS. Naturally, not all loops are perfectly identical, and deviations can lead to different vehicle behaviours, such as battery energy depletion or overcharging and poor performance in cabin temperature control. To address this limitation, the base policy provided by DP should accommodate various working conditions.

Being ref the solution of a random bus loop in the considered route solved by DP, as presented in previous paragraphs, this solution provides the optimal cost-to-go from any state x_j at time-step k expressed by $\mathcal{J}^*(x_j,k)_{ref}$ for this specific loop. Since the loops preserves the same covered distance, a space-based optimal cost-to-go is built. In this sense, a matrix $\mathcal{J}^*(x_j,s_i)_{ref}$ is generated by mapping the optimal cost-to-go in the reference cycle at a given vehicle position in the loop (s_i), depending on its states (SoE, T_{cab}). Therefore, considering that the driving cycles presents similarities of the same bus route, $\mathcal{J}^*(x_j,s_i)_{ref}$ provides an approximation of the optimal cost-to-go from any state x_j in the bus position s_i to any loop in the route. Next, rewriting the HJB Eq. (22) in the space base:

$$u_k = argmin_u \{L(x_k,w_k,u) + \mathcal{J}^*(f_k(x_k,u), s_{k+1})_{ref}\} \quad (24)$$

where f_k is the discrete version of the state function f in Eq. (18b) and $\mathcal{J}^*(f_k(x_k,u), s_{k+1})_{ref}$ is an estimation of the optimal cost-to-go from the state in the next time step, that is obtained from the DP solution of the reference cycle. Once $\mathcal{J}^*(x_j,s_i)_{ref}$ is an estimation of $\mathcal{J}^*(x_j,k)$, it is computed using a previous loop. So, the proposed algorithm generates a suboptimal solution, and the difference tends to decrease as the reference cycle approaches the real one to be covered. These differences between each bus trip can be attributed to varying traffic scenarios influenced by factors such as time of day, driver behavior, or uncertainties encountered by the bus along the route. This expression also suggests that a predicted driving cycle obtained through other predictive techniques can be utilized within the proposed approach.

The methodology proposed is demonstrated for the HEV model outlined in Section 3, which focuses on the energy management of a hybrid electric urban bus covering a specific route. However, this strategy can be extended to different powertrain architectures. To do so, two essential elements are necessary. Firstly, a high-fidelity model to represent the vehicle must accurately capture the impact of control actions evaluated across the grid generated in the optimization problem. Additionally, reliable driving cycle prediction is essential. In the present case, a previously covered cycle was used, but this approach can be extended to any estimated cycle.

Through the observation of Eq. (24), two statements can be highlighted:

- The proposed strategy can improve the base one since it employs information from the actual cycle in the next time-step (w_k) to determine u_k.
- Once this equation is evaluated each time step, the algorithm can employ the feedback of the current system states to adapt the control policy. For instance, avoiding battery SoE excursions out of the desired range and cabin temperatures away from setpoint.

Fig. 6 shows the diagram of the proposed strategy detailed for the case study. First, taking into account that the complete driving cycle consists of a sequence of similar loops, one loop previously covered by the bus is solved by offline DP optimization and used as a reference loop, and the cost-to-go obtained by this solution is stored in a map in the Reference cycle block. This map allows to estimate, through interpolation, the minimum cost to complete the trip at any position in the route considering the actual states and position of the bus $\mathcal{J}^*(\bar{SoE}, \bar{T}_{cab}, \bar{s})_{ref}$. Second, the

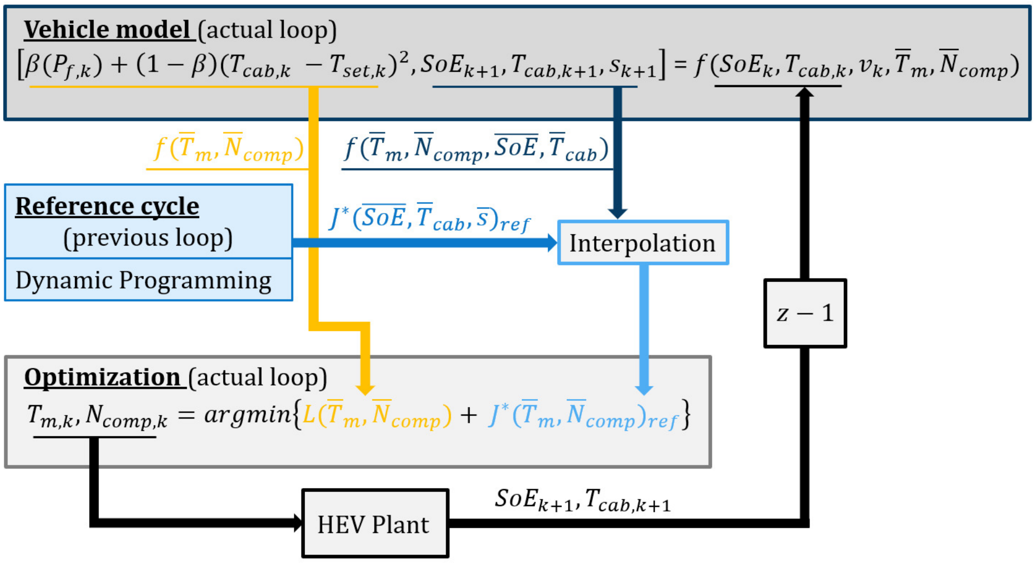

Figure 6. Block diagram of the proposed strategy.

real-time algorithm that runs while the bus covers the actual loop at every time step consists of the Vehicle model block and the Optimization block. In the Vehicle model block, the control-oriented model described in the previous section is employed to estimate the system states evolution depending on the set of possible combinations of controls action ($\bar{T}_m$ and $\bar{N}_{comp}$).

Simultaneously, this set of control candidates is evaluated in the generic cost function that balances the fuel consumption and cabin comfort according to the value assigned to β, providing the cost L. So the states estimated are used to interpolate in the cost-to-go map the minimum fuel consumption that the vehicle will consume from the next time-step to the end of the loop depending on the set of control candidates $\mathcal{J}^*(\bar{T}_m, \bar{N}_{comp})_{ref}$. Finally, in the Optimization block, the controls to be applied in the vehicle plant are the combination of both that minimizes the sum of the current cost (L), and the cost from the next time-step to the end ($\mathcal{J}^*$). Next, these control actions are applied to the HEV plant, updating the system states and then repeating this process until the end of the loop.

6 Results and discussion

6.1 Complete route analysis

In order to evaluate and compare the performance of the proposed strategy, a benchmark was performed. The EMS used to compare is the widespread ECMS. This approach relies on calibrating the λ factor to provide near-optimum results. To do that, a reference loop of the bus route (chosen at random) is employed to calibrate this factor and applied during the next loops. The same reference cycle was performed in the offline DP optimization to generate the cost to go matrix employed in the rollout algorithm. Since exists difference between this reference loop and the rest, the ECMS can fail in its aim of sustaining the charge. To avoid this problem, a feedback from the SoE was used, applying corrections close to the upper and lower limits of 0.3 and 0.7, respectively. Regarding the HVAC system control, the ECMS employs a rule-based control strategy, as typically embedded in automotive applications. This control strategy uses a PI to control the fan power that blows air to the cabin, passing the air through the evaporator to maintain the cabin temperature at 22 ºC. Another PI is used to control the compressor speed, aiming to keep the air temperature after the evaporator at 5ºC.

The upper plot of Fig. 7 presents the evolution of the system states for both approaches, considering the complete covered route on two consecutive working days. The first cycle is employed as the reference loop to calibrate the λ parameter, assuming full knowledge of the complete driving cycle. Then, it is iteratively tested until finding the value that provides the final SoE is equal to the initial one. Equally, the off-line DP optimization is applied to this reference loop to provide the cost-to-go matrix employed in the proposed strategy in the following loops to be covered.

An important aspect of the rollout algorithm is the influence of the β parameter on the problem states. This parameter can balance the cost function evaluated in the EMS, prioritizing the minimization of fuel consumption or cabin temperature deviation about the setpoint. The impact of this parameter is discussed in the next section. However, in this case, the value assumed for the parameter that balances the terms in Eq. (17) was β=0.85. It is noticed that the proposed strategy success in keeping the SoE in the allowed range along the complete route. On the other hand, the λ factor in the ECMS calibrated with the same information available from the reference cycle frequently hits the SoE limits, being able to keep its value close to the desired range due to the corrections applied to λ. Additionally, regarding cabin temperature control, it is possible to note that both strategies controlled the temperature between 24.5 and 19.5 ºC throughout the entire cycle.

In the case at hand, the first cycle was used as a reference to calibrate the λ and to use it in the DP offline optimization. The lower left part of Fig. 7 shows the evolution of the states for this reference cycle, where the disturbances and the complete driving cycle are assumed to be the information obtained by de bus covering a previous loop. The similarity

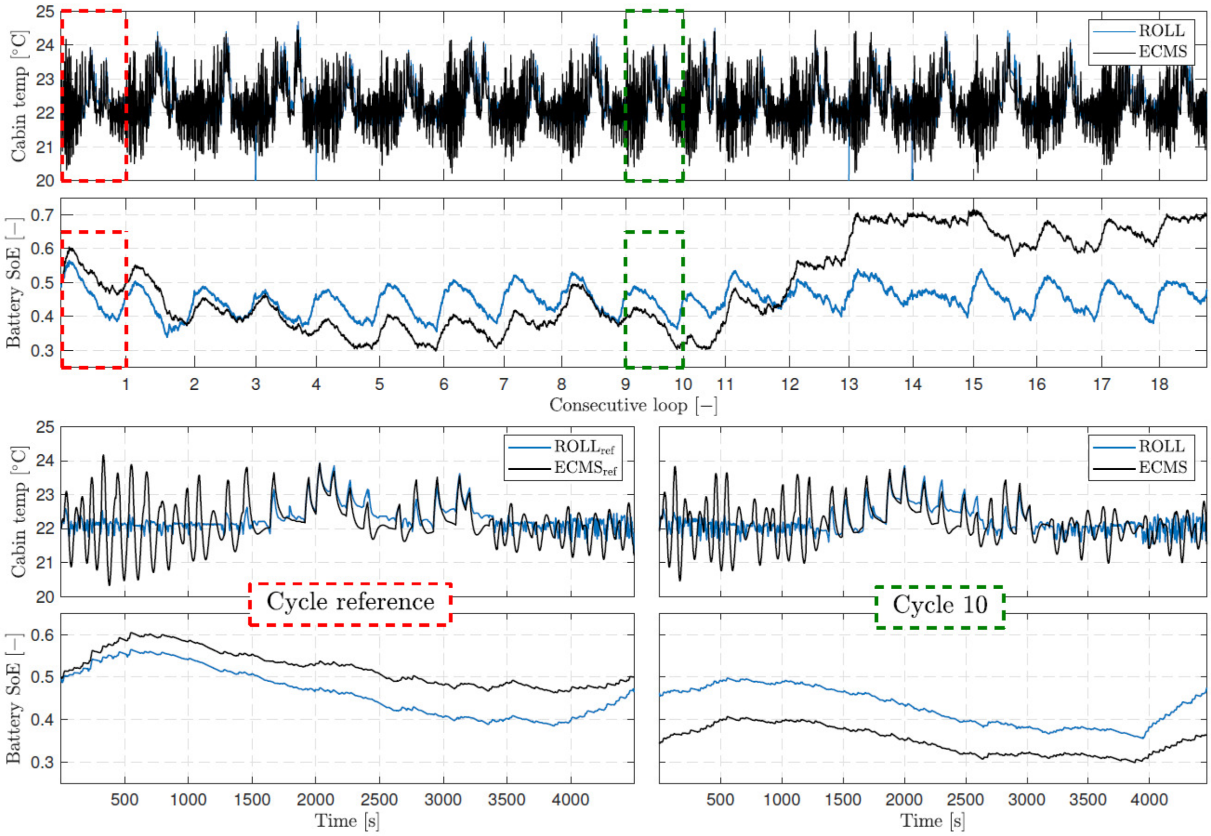

Figure 7. Comparison between the complete route evaluated with the proposed and the standard approach presenting the SoE and cabin temperature evolution (upper). Analysis of a single loop regarding the reference cycle used to calibrate both strategies and a given loop in the middle of the route (bottom).

between the SoE evolution of this particular loop can be explained by the fact that both strategies employ optimal control techniques to solve the EMS problem. The ECMS is based on Pontryagin's minimum principle, and the rollout exploits a DP solution of the cycle at hand.

Regarding the cabin temperature control performance, the ECMS does not have a particular strategy, employing PIs to control the HVAC airflow and the compressor speed. Additionally, the rollout uses the same PI to control de HVAC air flow, but the compressor speed is modeled as a control action in the proposed approach. Analyzing the cabin temperature evolution for the ECMS case, the oscillation observed is related to the PIs implemented in the standard cabin temperature control. Moreover, the evolution noticed by the Rollout can maintain the cabin temperature closer to the setpoint. Both strategies experiment with a temperature increase close to the middle of the loop because this region is the condition where more passengers are inside the bus. Even though the HVAC works close to the maximum power, the temperature presented a significant deviation concerning the setpoint.

The analysis of the route covered by the bus shows that in the first reference loop, both strategies are able to maintain the states close to the desired range since they explore the perfectly known driving conditions. However, as far as the bus travels the following loops, where the driving disturbances are unknown, the proposed method shows to be more robust than the ECMS. So comparing the performance of a loop in the middle of the route (cycle 10), the right bottom part of Fig. 7 shows the states evolution. This chosen cycle represents a situation where both strategies employ just the information available from the reference cycle in the EMS to provide the inputs to the vehicle plant in a different set of disturbances and driving cycle. The cabin temperature shows the same behavior as the reference cycle, so being able to control it near the setpoint. The SoE of the ECMS case demonstrates that only calibrating the λ for a given reference cycle is insufficient to keep the it within the allowed range.

To explore the strategies under varied scenarios, the entire route was reassessed using a different bus loop as the reference cycle, generating the cost-to-go matrix for the rollout and calibrating the λ parameter of the ECMS. The evolution of T_{cab} and SoE across the entire route is depicted in Fig. 8. Both strategies demonstrated comparable performance in controlling cabin temperature. However, concerning the SoE evolution, the ECMS managed to maintain it within the desired range until approximately the sixth loop, after which it frequently exceeded the upper limit.

Based on the comparative performance of both strategies, it is evident that the proposed approach has the potential to outperform the standard ECMS. While both methods share identical calibration requirements involving optimizing a reference cycle, the ECMS consolidates all information from the reference cycle into a single parameter, λ. In contrast, the rollout strategy leverages the entirety of the cost-to-go from the reference cycle. As a result, the control

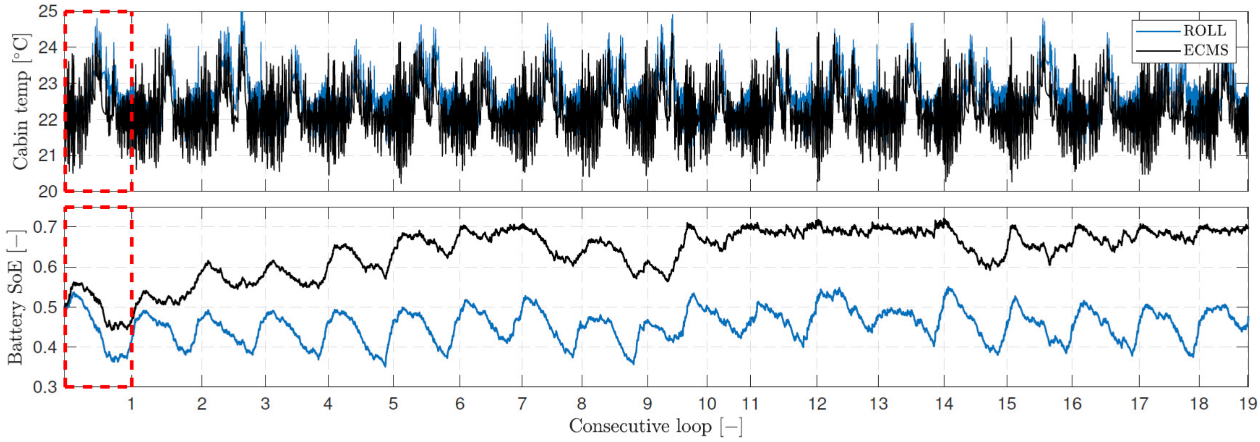

Figure 8. Comparison between the complete route evaluated with the proposed employing a different reference cycle to calibrate the strategies.

policy employed by the ECMS approach relies solely on a single constant, with minimal dependency on the system state, except for the SoE correction in values outside the allowed range (0.3 and 0.7). Conversely, the rollout strategy adopts a more comprehensive approach that considers the influence of system states (SoE and $Tcab$) and vehicle position in the control policy. However, this enhanced EMS comes at the cost of more significant storage requirements, dependent on the size of the problem. For instance, in the current scenario, where $\mathcal{J}^*(x_j, s_i)_{ref}$ has a size of 305 x 101 x 101, representing a discretization in SoE of 101 points between 0.3 and 0.7, 101 points between 19 and 26 °C in T_{cab}, and a 50 m discretization of the 15.1 km loop distance.

6.2 Calibration of β parameter

For this part of the analysis, the influence of the parameter β is discussed, to do that, the complete route presented in the Fig. 8 is employed. This route was covered by the ECMS case taken as a reference for the comparison, and the parameter β was evaluated for the set of values as (0.95 0.9 0.85 0.8 0.7).

The states and the total fuel consumption of one single loop in the middle of the considered route are presented on Fig. 9. The cases $\beta = 0.95$ and $\beta = 0.7$ represent two extremes of the proposed strategy, and the standard approach is the ECMS. So, comparing the cabin temperature, as expected, low β can maintain the cabin temperature close to setpoint, while high β allows the temperature to vary while keeping the temperature within limits defined in the cost function. Also, close to the middle of the loop is the condition where more passengers are inside the bus, and even under these conditions, it was observed that the lowest beta can keep the temperature closer to the setpoint. Of course, this improvement in cabin temperature control performance comes at the cost of an increase in fuel consumption. Consequently, the β states one optimization criteria that, as exposed in Eq. (17), balances the cost function employed in the EMS, attributing lower or higher penalties to the terms that evaluate the fuel consumption of the engine and the cabin temperature deviation from the setpoint.

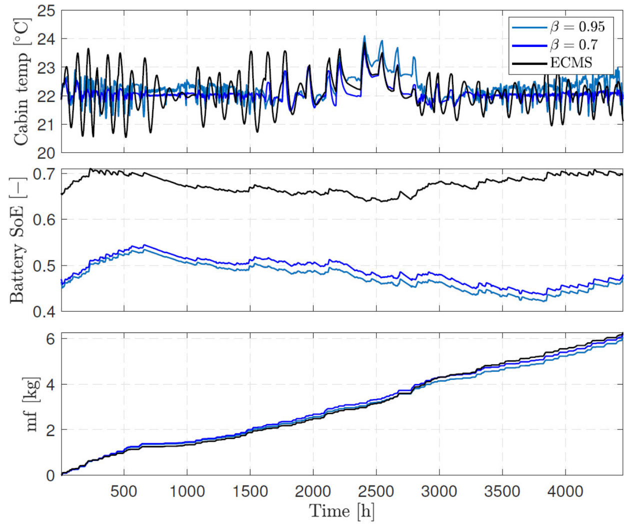

Figure 9. Representation of states and fuel consumption of a single loop employing the ECMS and the proposed strategy varying the β parameter.

On the other hand, regarding the SoE evolution, for both the values of β, it is clear that it can maintain the state of charge close to 0.5, achieving the charge sustaining operation. Also, they presented a similar profile because both employed the same EMS. Please note that the term Φ in Eq. (18e) penalizes deviations from the desired final state at the end of the loop. That is, increasing this penalty can also guarantee that the final state of charge will be very close to a desired setpoint in this case 0.5. Moreover, even though the ECMS had the λ calibrated with a loop of the bus in the same route, the standard strategy is not able to keep the SoE close to the desired level.

As stated before, this study aims to control cabin temperature by addressing the optimization of passengers comfort and fuel consumption. By doing so, it is possible to reduce overall energy consumption by controlling the HVAC power consumption. So, Fig. 10 shows the HVAC performance of the set of β regarding the standard ECMS. In the upper plot, the discomfort ratio is defined as the sum of the difference between cabin temperature and the lower and upper limits (21 and 23 °C) for the total

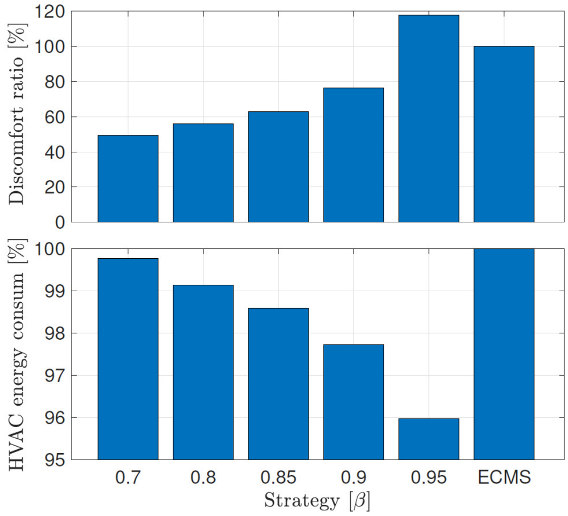

Figure 10. HVAC energy consumption and discomfort ratio varying the Beta parameter regarding the standard ECMS strategy.

trip covered. Equally, at the bottom plot is presented the total HVAC energy consumption. It can be noticed that for values of β from 0.7 to 0.9, the proposed strategy can improve cabin temperature control without penalizing energy consumption. The results show that the best scenario of $\beta = 0.70$ presented a 50% reduction in the discomfort ratio presenting approximately the same energy consumption as the baseline strategy. Also, a decrease of 4% in the total HVAC energy consumption was noticed for $\beta = 0.95$, but increasing the discomfort ratio to 20%.

Fig. 11 summarizes the results in a pareto front for the complete route evaluated by the standard EMCS and the set of β performed regarding the total fuel consumption and the discomfort ratio. Analysing this figure is noticeable that a trade-off exists between fuel consumption and cabin temperature comfort. In terms of fuel consumption, it can be highlighted that the iso fuel consumption reduces by almost 50% the cabin discomfort, and the iso discomfort can reduces fuel consumption by 1.5%.

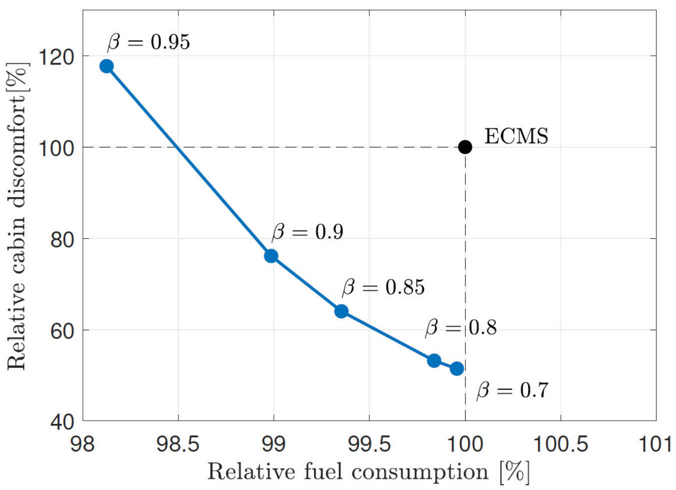

Figure 11. Pareto frontier of the proposed strategy in comparison with the results obtaines with the standard ECMS strategy for the complete route.

7 Conclusions

This article addresses the problem of an urban electric urban bus covering two consecutive daily commutes. The proposed strategy employs the information available from previously covered loops in the same bus route to optimize the energy management strategy of the following loops. The novelty of this work is based on using information from a cycle previously recorded to provide an optimal solution of a reference cycle, then generating a cost to be employed in the online optimization. Whereas approaches in the literature typically use methods to estimate future driving conditions. The energy management strategy actuates in the power split between the ICE and the motor and in the HVAC system by controlling the cabin temperature considering the variation in the number of passengers on the bus. In the end, a benchmark has been carried out to compare the performance of the proposed energy management strategy with a standard ECMS widespread algorithm for HEV energy management, embedded with rule-based strategies to control the HVAC system. The main contributions of this work can be summarized as follows:

(i) The proposed EMS does not rely on estimating future driving conditions or the number of passengers on the bus but rather on exploring information from previously covered loops.
(ii) A strategy based on an optimization criterion was developed, balancing the compromise between fuel consumption and the performance of cabin temperature control.
(iii) The pareto front allows to compare different EMS calibrations concerning the β chosen, presenting the trade-off between discomfort ratio and fuel consumption.
(iv) The results compared to the standard strategy shows that it was possible to reduce the discomfort ratio by up to 45% with the same fuel consumption or decrease it by 20% and while provide fuel economy by 1%.

8 Funding

This research was funded by Ministerio de Ciencia e Innovación, through the Proyectos I+D+i 2020 Program, grant number PID2020-119691RB-I00.

References

1. IEA. Transport Improving the sustainability of passenger and freight transport. Accessed 23-03-2023. 2022 3.
2. Nanaki EA. Electric vehicles for smart cities: trends, challenges, and opportunities. 2020.
3. Climent H, Pla B, Bares P, Pandey V. Exploiting driving history for optimising the Energy Management in plug-in Hybrid Electric Vehicles. Energy Conversion and Management. 2021;234.
4. Zhuang W, Eben SL. A survey of powertrain con fi guration studies on hybrid electric vehicles. Applied Energy. 2020;262(October 2019):114553.
5. Hu X, Han J, Tang X, Lin X. Powertrain Design and Control in Electrified Vehicles: A Critical Review. IEEE Transactions on Transportation Electrification. 2021;7(3):1990-2009.

6. Podder AK, Chakraborty O, Islam S, Kumar NM, Alhelou HH. Control strategies of different hybrid energy storage systems for electric vehicles applications. IEEE Access. 2021;9:51865-95.
7. Tian Z, Qian C, Gu B, Yang L, Liu F. Electric vehicle air conditioning system performance prediction based on artificial neural network. Applied Thermal Engineering. 2015;89:101-14.
8. Onori S, Serrao L, Rizzoni G. SPRINGER BRIEFS IN ELECTRICAL AND COMPUTER Hybrid Electric Vehicles Energy Management Strategies; 2016.
9. Xiao R, Liu B, Shen J, Guo N, Yan W, Chen Z. Comparisons of energy management methods for a parallel plug-in hybrid electric vehicle between the convex optimization and dynamic programming. Applied Sciences (Switzerland). 2018;8(2):16-9.
10. Tran DD, Vafaeipour M, El Baghdadi M, Barrero R, Van Mierlo J, Hegazy O. Thorough state-of-the-art analysis of electric and hybrid vehicle powertrains: Topologies and integrated energy management strategies. Renewable and Sustainable Energy Reviews. 2020;119:109596.
11. Li Z, Khajepour A, Song J. A comprehensive review of the key technologies for pure electric vehicles. Energy. 2019;182:824-39.
12. Lew A, Mauch H. Dynamic programming: A computational tool. vol. 38. Springer; 2006.
13. Schmid R, Bürger J, Bajcinca N. A comparison of PMP-based Energy Management Strategies for Plug-in-Hybrid Electric Vehicles. IFAC-PapersOnLine. 2019;52(5):592-7.
14. Harselaar WV, Schreuders N, Hofman T, Rinderknecht S. Improved Implementation of Dynamic Programming on the Example of Hybrid Electric Vehicle Control. IFAC-PapersOnLine. 2019;52(5):147-52.
15. Feng J, Han Z. Progress in Research on Equivalent Consumption Minimization Strategy Based on Different Information Sources for Hybrid Vehicles (Mar. 2023). IEEE Transactions on Transportation Electrification. 2023:1-1.
16. Zhao S. A Study on Adaptive Power Split Strategy of HEV Using Nonlinear System Identification; 2021.
17. Shi D, Li S, Liu K, Xu Y, Wang Y, Guo C. Adaptive energy management strategy for plug-in hybrid electric vehicles based on intelligent recognition of driving cycle. Energy Exploration & Exploitation. 2023;41(1):246-72.
18. Li X, Han L, Liu H, Wang W, Xiang C. Real-time optimal energy management strategy for a dual-mode power-split hybrid electric vehicle based on an explicit model predictive control algorithm. Energy. 2019;172:1161-78.
19. Huang Y, Wang H, Khajepour A, He H, Ji J. Model predictive control power management strategies for HEVs: A review. Journal of Power Sources. 2017;341:91-106.
20. He H, Yan M, Sun C, Peng J, Li M, Jia H. Predictive air-conditioner control for electric buses with passenger amount variation forecast. Applied energy. 2018;227:249-61.
21. Khayyam H, Kouzani AZ, Hu EJ, Nahavandi S. Coordinated energy management of vehicle air conditioning system. Applied Thermal Engineering. 2011;31(5):750-64. MNF 2009 Special Issue.
22. Amini MR, Gong X, Feng Y, Wang H, Kolmanovsky I, Sun J. Sequential optimization of speed, thermal load, and power split in connected hevs. Proceedings of the American Control Conference. 2019;2019-July:4614-20.
23. Amini MR, Wang H, Gong X, Liao-McPherson D, Kolmanovsky I, Sun J. Cabin and Battery Thermal Management of Connected and Automated HEVs for Improved Energy Efficiency Using Hierarchical Model Predictive Control. IEEE Transactions on Control Systems Technology. 2020;28(5):1711-26.
24. Sommer M, Sax E, Rösch T. Model Predictive HVAC Control with disturbance variable forecasting for city buses. In: 2021 International Conference on Electrical, Computer, Communications and Mechatronics Engineering (ICECCME). IEEE; 2021. p. 1-7.
25. Hu Q, Reza Amini M, Wiese A, Tascillo M, Buckland Seeds J, Kolmanovsky I, et al. A Spatial Data-Driven Vehicle Speed Prediction Framework for Energy Management of HEVs Using Multi-Horizon MPC with Non-uniform Sampling. In: 2022 American Control Conference (ACC); 2022. p. 1024-9.
26. Tormos B, Pla B, Bares P, Pinto D. Energy Management of Hybrid Electric Urban Bus by Off-Line Dynamic Programming Optimization and One-Step Look-Ahead Rollout. Applied Sciences. 2022;12(9):4474.
27. Pinzon JA, Vergara PP, da Silva LCP, Rider MJ. Optimal Management of Energy Consumption and Comfort for Smart Buildings Operating in a Microgrid. IEEE Transactions on Smart Grid. 2019;10(3):3236-47.
28. ASHRAE. ASHRAE Handbook - Fundamentals. Atlanta, GA: ASHRAE; 2017.
29. Cho H, Liu B, Gowri K. Energy saving impact of ASHRAE 90.1 vestibule requirements: Modeling of air infiltration through door openings. Pacific Northwest National Lab.(PNNL), Richland, WA (United States); 2010.
30. Guzzella L, Sciarretta A, et al. Vehicle propulsion systems. vol. 1. Springer; 2007.
31. Li H, Zhou Y, Xiong H, Fu B, Huang Z. Real-time control strategy for CVT-based hybrid electric vehicles considering drivability constraints. Applied Sciences. 2019;9(10):2074.
32. Bertsekas D. Rollout algorithms for constrained dynamic programming. Lab for Information and Decision Systems Report. 2005;2646.
33. Lewis FL, Syrmos V. L. 1995 Optimal Control; 1995.